Proceedings of the 17th World Congress
The International Federation of Automatic Control
Seoul, Korea, July 6-11, 2008

Robust Fault Diagnosis of Energetic System with Parameter Uncertainties

M. A. Djeziri * B. Ould Bouamama and R. Merzouki **

* LAGIS, UMR CNRS 8146, Ecole Centrale de Lille, BP 48, 59651 Villeneuve d'Ascq Cedex, France.
** LAGIS, UMR CNRS 8146, Ecole Polytechnique de Lille, Avenue Paul Langevin 59655 Villeneuve d'Ascq, France.
(e-mail: mohand.djeziri@polytech-lille.fr).

Abstract: In this paper, a bond graph model based approach for robust FDI (Fault Detection and Isolation) in presence of parameter uncertainties is presented. Due to the energetic and multi physical properties of the Bond Graph, the whole of nonlinear model, structural analysis, residual with adaptive thresholds generations, and residual sensitivity analysis, can be synthesized using only one tool. This method is applied online for industrial steam generator. Experimental results are given to support the theoretical development.

keywords: Steam Generator, Bond Graph, Parameter Uncertainties, FDI, Linear Fractional Transformations, Sensitivity Analysis.

1. INTRODUCTION

Recently, robust fault diagnosis has been the subject of several researches, due to the increase of system complexity, and the industrial requirement around the safety and the yield. FDI (Fault Detection and Isolation) procedures consist of comparison between the actual process behavior and the theoretical reference process behavior, represented by its mathematical model. In literature, two fault diagnosis approaches exist: quantitative and qualitative. Among works published these last years on the robust diagnosis using these approaches, one can find: (*M. Basseville (1998)* [4]), (*O. Adrot & al. (1999)* [1]), (*J. Armengol & al.(2000)* [2]), (*Z. Han & al. (2002)* [8]), (*K. Hising-Chia & al. (2004)* [10]), (*D. Henry & al. (2005)* [9]).

Due to the bond graph' behavioral, structural and causal properties, this tool is more and more used for modelling and fault diagnosis. From FDI point of view, the causal properties of the bond graph tool were initially used for the determination of the faults' origin. For an electromechanical system application, FDI scheme is proposed in (*M. A. Djeziri & al. (2006)* [5]), in order to detect the presence of a perturbed backlash phenomenon, in presence of parameter uncertainties. These latter are assumed as normally distributed' Gaussian signals with zero mean and a known variance. In (*M. A. Djeziri & al. (2007)* [6]), the normalized gradient method is applied in real time on an electromechanical test bench for parameter and uncertainties identifications.

In this paper, a bond graph methodology is used to synthesis a robust FDI method for nonlinear system in presence of parameter uncertainties, and tested on an industrial steam generator. This FDI method is summarized by the following steps:

· Modeling of studied system using bond graph tool with standard LFT form; · Generation of Analytical Redundancy Relations (ARRs) from the uncertain model by decoupling the nominal and the uncertain parts. Residuals correspond to the ARR nominal part, while their adaptive thresholds represent the ARR uncertain parts; · Residual' sensitivity analysis is done by using the ARR uncertain part, in order to calculate the fault detectability indices.

This paper is organized as follows: Section 2 presents briefly the LFT form modelling and its advantages for robust diagnosis. In Section 3, the bond graph LFT modelling of the steam generator in presence of parameter uncertainties is given. Section 4 describes the robust ARRs generation algorithm and the residual sensitivity analysis. The experimental results are shown in Section 5. Finally, conclusion is given in Section 6.

2. LFT AND ROBUST DIAGNOSIS

The main advantages of the bond graph model in LFT form for robust diagnosis, are given as follows:

· Introduction of the uncertainties on the nominal model, does not affect the causality and the structural properties of the BG elements;

· Representation of all uncertainties (*i.e.* structured and unstructured);

· Uncertain part is perfectly separated from the nominal part;

· Parameter uncertainties are easily evaluate.

3. UNCERTAIN MODELING OF THE STEAM GENERATOR SYSTEM

The steam generator proposed for this application is a complex and non stationary energetic system. This process

⋆ This research was supported by the Europeen framework project FP6 'CHEM' and the Regional funded project ARCIR 2004-2007.

can be decomposed in three principal subsystems: The tank, the pump with a pipe and the boiler.

3.1 Modeling hypothesis

The steam generator is modeled by considering the following hypothesis:

· Water and steam are supposed in thermodynamic equilibrium state, due to their good emulsion homogenization;

· Boiler mixture is considered under uniform pressure;

· Steam generator has a heat capacity and sudden a heat losses by conduction towards external environment;

· Fluid in the feeding circuit is incompressible.

3.2 The tank

Determinist and uncertain bond graph models of the tank are respectively given in Fig.1-(a) and (b). The storage of hydraulic and thermal energies is modelled respectively by the bond graph elements $C : C_h$ and $C : C_t$. The input mass flow $Sf : \dot{m}_{in}$ is assumed equal to zero and the tank is initially full fill-in. Then the following equation is deduced from the junction 0_h of the bond graph determinist model in derivative causality:

$$\dot{m}_{out} = -C_h.\frac{dP_1}{dt} \tag{1}$$

where $\dot{m}_{out}$ is the tank output' mass flow, C_h represents the hydraulic capacity of the tank, P_1 is the fluid pressure measurement inside the tank. Knowing that the studied tank is cylindrical, C_h can be expressed as follows:

$$C_h = A_T.(\rho_T.g)^{-1} \tag{2}$$

where A_T is the tank section, ρ_T is the fluid density which is function of the fluid pressure and g is the gravity acceleration.

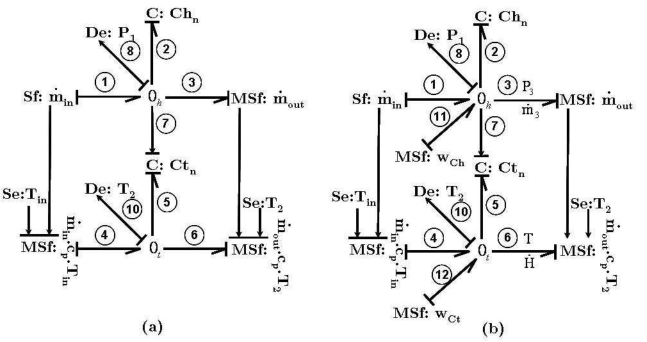

Fig. 1. (a): Tank determinist model. (b): Tank uncertain model.

The uncertainty on C_h noted δ_{C_h} corresponds to the whole of uncertainty on the tank section A_T, and uncertainty on the fluid density ρ_T. δ_{A_T} is due to the extra thicknesses of corrosion, and its value with nominal value A_{Tn} are given by the manufacturer. The fluid density function ρ_T is calculated using polynomial interpolation method, and the uncertainty $\delta_{\frac{1}{\rho_T}}$ is equal to the estimation error given by this polynomial interpolation.

The relation between C_{h_n} and δ_{C_h} is given by the following expression:

$$C_h = C_{hn} + \delta_{C_h}.C_{hn} \tag{3}$$

where C_{h_n} is the nominal value of C_h.

The modulated input w_{C_h} in Fig.1 corresponds to an effort variable deduced from δ_{C_h} and expressed by the following equation:

$$w_{C_h} = -\left(\delta_{\frac{1}{\rho_T}} + \delta_{A_T} + \delta_{A_T}.\delta_{\frac{1}{\rho_T}}\right).\frac{A_{T_n}}{\rho_{T_n}.g}.\frac{dP_1}{dt} \tag{4}$$

w_{C_h} is taken with a negative sign, because it is considered as a fictive flow input' source (Fig.1).

Since the input mass' flow is assumed equal to zero, the energetic assessment calculated from the junction 0_t, on the determinist model of Fig.1 is given as follows:

$$\dot{H}_5 = -\dot{m}_{out}.c_p.T_2 \tag{5}$$

where $\dot{H}_5$ is the enthalpy flow at the output of the $C : C_t$ element, c_p is the fluid specific heat at constant pressure, and T_2 is the sensor measurement of the fluid temperature inside the tank.

The uncertainty on the enthalpy flow $\dot{H}_5$ is due to the uncertainty δ_{C_t} on the C_t parameter. This uncertainty is issued from the variation of the fluid specific heat at constant pressure c_p, which is also in function of the fluid temperature. The nominal value c_{p_n} and its uncertainty δ_{c_p} are calculated using the polynomial interpolation algorithm, then the uncertainty on C_t element is calculated as follows:

$$w_{Ct} = -\delta_{c_p}.(\dot{m}_{out}.c_{p_n}.T_2) \tag{6}$$

3.3 Pump with pipe

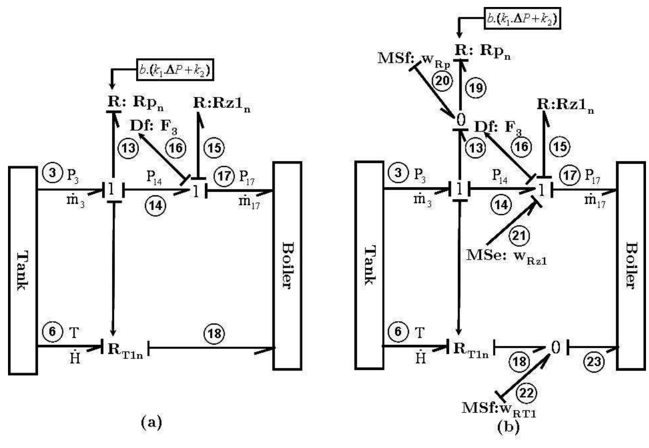

Fig. 2. (a): Pump and pipe determinist model. (b): Pump and pipe uncertain model.

In bond graph models of Fig. 2, the pump and pipe are represented separately by two resistances. The pump is modeled by a resistance *Rp* and modulated by the pump characteristic of equation (7). This latter describes the relation between the pressure $\Delta P = P_{14} - P_3$ and the mass flow generated by the pump $\dot{m}_{14}$..

$$\dot{m}_{14} = b.(k_1.(P_{14} - P_3) + k_2) \tag{7}$$

P_3 and P_{14} are respectively the input and output pressures of the pump. k_1 and k_2 are the pump characteristic parameters. b is the boolean control parameter.

The modulated source $MSf : w_{Rp}$ on the bond graph model of Fig. 2-(b) represents the uncertainty on the mass flow at the pump output and is given by the following expression:

$$w_{Rp} = -\left[\delta_{k_1}.(k_{1_n}.(P_{14} - P_3) + \delta_{k_2}.k_{2_n}\right] \tag{8}$$

The flow parameter Rz_1 depends on the tubing details and is a function of the valve opening. The nominal value of Rz_1 and its uncertainty can be calculated using equation (9), where the *Poiseuille* flow case is considered.

$$\begin{aligned} Rz_1 &= \frac{8.\rho_l.L_p}{\pi.r_{1p}} \\ \delta_{Rz_1} &= \delta_{\rho_l}.\delta_{L_p}.\delta_{\frac{1}{r_{1p}}} + \delta_{\rho_l} + \delta_{L_p} + \delta_{\frac{1}{r_{1p}}} + \delta_{\rho_l}.\delta_{L_p} \\ &\quad + \delta_{\rho_l}.\delta_{\frac{1}{r_{1p}}} + \delta_{L_p}.\delta_{\frac{1}{r_{1p}}} \end{aligned} \tag{9}$$

with L_p is the pipe length and $r_{1p} = {r_p}^4$, where r_p is the pipe radius.

The mass flow $\dot{m}_{17}$ is calculated using the *Bernoulli* law:

$$\dot{m}_{17} = \frac{1}{R_{z_1}}.\sqrt{P_{14} - P_{17}}$$

Then, the uncertainty on the effort at the output of the pipe is determined as follows:

$$w_{Rz_1} = -\left(\delta_{Rz_1} + 2.\delta_{Rz_1}\right).(Rz_{1n}.\dot{m}_{17})^2 \tag{10}$$

with Rz_{1n} and δ_{Rz_1} are respectively the nominal value and multiplicative uncertainty value of the flow parameter R_{Z1}. F_3 is the mass flow measurement given by the detector $Df : F_3 = \dot{m}_{17}$

The enthalpy flow through the pipe is convected by the fluid as follows:

$$\dot{H}_{13} = T_6.c_p.\dot{m}_3 \tag{11}$$

The coupling of thermal and hydraulic energies is modelled by a multiport element $R : R_{T1}$. The variables $\dot{m}_3$ and T_6 are measured respectively by the F_3 and T_2 sensors

The uncertainty on the thermal energy transmitted by the pump to the boiler is due to the variation of the specific heat at constant pressure c_p according to the fluid temperature. This last temperature is assumed as a variation between the temperature of the water in the tank and the ambient temperature Ta. It is expressed by the following equation:

$$w_{R_{T1}} = -\delta_{c_p}.(T_2.c_{p_n}.F_3) \tag{12}$$

3.4 The boiler

Determinist and uncertain bond graph models of the boiler are given in Fig. 3-(a) and (b)

The storage of hydraulic and thermal energies is modelled by the two ports element $C : C_{ht}$. The thermal energy stored by the boiler wall is modeled by a simple one port C element, and the heat transfer from the boiler to the environment is modeled by $R : R_a$ element. The

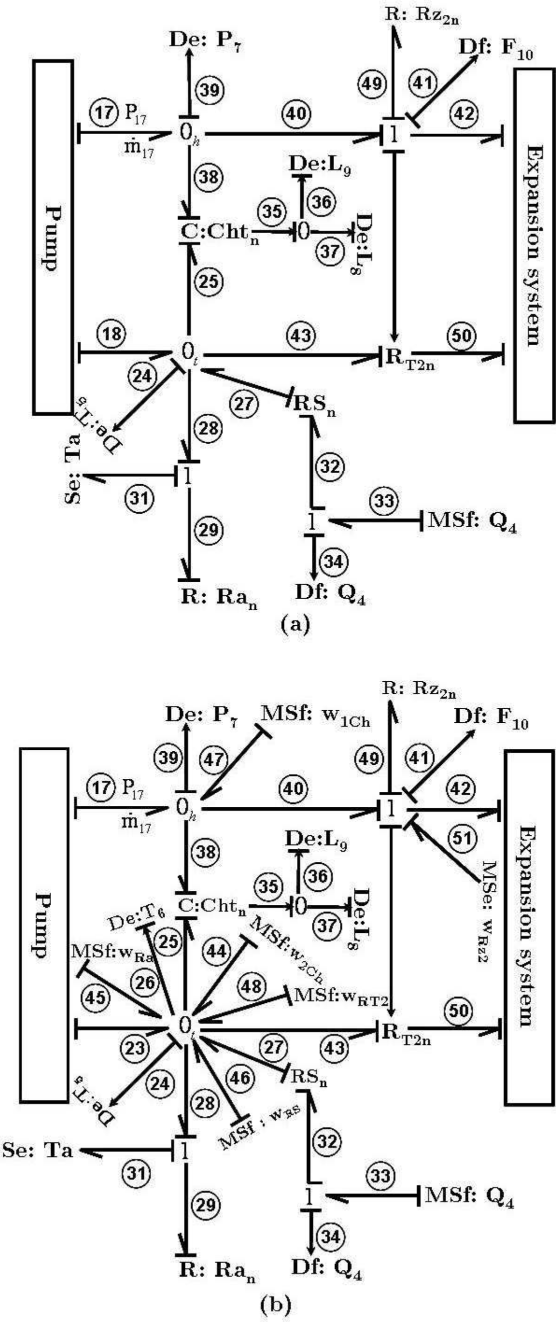

Fig. 3. (a): Boiler determinist model. (b): Boiler uncertain model.

boiler is instrumented with two redundant sensors of temperature($De : T_5 and De : T_6$), two redundant volume sensors $(De : L_8 and De : L_9)$, a pressure sensor $(De : P_7)$, a mass flow sensor at the output of the boiler $(Df : F_{10})$, and a sensor of the power provided to the thermal resistor $(Df : Q_4)$.

Dissipation of the heat flow $\dot{H}_{28}$ via the boiler wall can be determined using the thermal conductivity λ, thickness e_B, the difference between the the wall sides' temperature $T_b - T_a$ and the section A_B of the boiler wall, according to the following relation:

$$\dot{H}_{28} = \lambda.\frac{A_B}{e_B}.(T_b - T_a) \tag{13}$$

Where T_a and T_b are respectively the ambient and boiler temperatures. The heat transfer coefficient via the boiler wall is $Ra = \lambda.\frac{A_B}{e_B}$, where its uncertainty δ_{Ra} is the combination of δ_{A_B} and $\delta_{\frac{1}{e_B}}$.

Then the flow source $(MSf : w_{Ra})$ of Fig. 3-(b) which represents the uncertainty on the heat flow dissipated via the boiler wall is expressed as follows

$$w_{Ra} = -\delta_{Ra}.Ra_n.(T_5 - Ta) \tag{14}$$

The flow at the output of the $C : C_{ht}$ element represents the interaction of the mass flow $\dot{m}_{C_{ht}}$ and the heat flow $\dot{H}_{C_{ht}}$ in the boiler, given in the system of equations (15).

$$\begin{cases} \dot{m}_{C_{ht}} = \dfrac{d}{dt}\left(\rho_l.V_l + \rho_v.V_v\right) \\ \dot{H}_{C_{ht}} = \dfrac{d}{dt}\left(\rho_l.h_l.V_l + \rho_v.h_v.V_v - P_B.V_B\right) \end{cases} \tag{15}$$

where ρ_l, h_l, V_l and ρ_v, h_v, V_v are respectively the density, the specific enthalpy and the volume of water and steam inside the boiler. P_B is the boiler pressure given by the pressure measurement P_7, V_B is the known volume of the boiler.

All variables ρ_l, h_l, ρ_v and h_v are function of the pressure P_7 and calculated using a polynomial interpolation algorithm. δ_{ρ_l}, δ_{ρ_v}, δ_{h_l} and δ_{h_v} represent the the estimation errors of the polynomial interpolation algorithm.

Taken into account the uncertainties on the variables ρ_l, h_l, V_l, ρ_v, h_v and V_v, the uncertainties on the $C : C_{ht}$ element are given as follows

$$\delta_{1C_{ht}} = \delta_{\rho_l}.\delta_{V_l} + \delta_{\rho_l} + \delta_{V_l} + \delta_{\rho_v}.\delta_{V_v} + \delta_{\rho_v} + \delta_{V_v} \tag{16}$$

$$\delta_{2C_{ht}} = \delta_{1C_{ht}} + \delta_{h_l} + \delta_{V_l}.\delta_{h_l} + \delta_{\rho_l}.\delta_{h_l} + \delta_{\rho_l}.\delta_{V_l}.\delta_{h_l} \tag{17}$$

$$+\delta_{h_v} + \delta_{V_v}.\delta_{h_v} + \delta_{\rho_v}.\delta_{h_v} + \delta_{\rho_v}.\delta_{V_v}.\delta_{h_v} \tag{18}$$

where $\delta_{1C_{ht}}$ represents the hydraulic uncertainty on C_{ht}, and $\delta_{2C_{ht}}$ represents the thermal uncertainty on C_{ht}.

Then, the flow sources $MSf : w_{1C_{ht}}$ and $MSf : w_{2C_{ht}}$ are expressed by the following expressions:

$$\begin{cases} w_{1C_{ht}} = -\delta_{1C_{ht}}.\dfrac{d}{dt}\left(\rho_{l_n}.V_{l_n} + \rho_{v_n}.V_{v_n}\right) \\ w_{2C_{ht}} = -\delta_{2C_{ht}}.\dfrac{d}{dt}\left(\rho_{l_n}.h_{l_n}.V_{l_n} + \rho_{v_n}.h_{v_n}.V_{v_n}\right) \end{cases} \tag{19}$$

The bond graph element RS of Figs. 3-(a) and (b) represents the thermo-resistance, its nominal value RS_n and its uncertainty δ_{RS} are calculated using the electrical power given by the sensor Q_4. Then the flow source $MSf : w_{RS}$ which represents the uncertainty on the heat flow provided to the boiler is given in equation (20).

$$w_{RS} = -\delta_{RS}.\left(RS_n.Q_4\right) \tag{20}$$

According to model of Fig. 3-(a), the heat flow driven by the steam at the boiler output is given in equation (21).

$$\dot{H}_{43} = T_6.c_v.F_{10} \tag{21}$$

with c_v is the steam heat capacity at constant volume.

The uncertainty on the heat flow at the boiler output is due to the uncertainty δ_{c_v}, then the flow source $MSf : w_{RT_2}$ is modulated as follows:

$$w_{RT_2} = -\delta_{c_v}\left(T_6.c_{v_n}.F_{10}\right)$$

4. ROBUST ARRS GENERATION

The generation of the robust $ARRs$ from a proper and observable bond graph model is summarized in the following steps:

1^{st} *step*: The bond graph model is made in derivative causality with LFT form;

2^{nd} *step*: The unknown variables are eliminated by covering the causal paths from the bond graph elements to the detectors;

3^{rd} *step*: The $ARRs$ are generated by expressing energetic assessments on the junctions 1 and 0, where all the unknown connected variables are determined from the 2^{nd} *step*.

The energetic assessments is expressed by two fundamental laws for each junction:

Jonction 1:

$$f_1 = f_2 = f_3 = ...$$
$$ARR : \sum e_{i_n} + \sum w_i = 0 \tag{22}$$

for 0 *junction*, e_{i_n} is replaced by f_{i_n}

$i_n \in \{R_n, I_n, C_n, TF_n, GY_n, RS_n, MSe_n, MSf_n\}$,

$i \in \{R, I, C, TF, GY, RS, MSe, MSf\}$.

4^{th} *step*: The obtained ARRs at the 3^{rd} *step* are composed of two perfectly separate parts, a nominal part called r which describes the residual, and an uncertain part called a, represents the sum of fictive input values $\sum w_i$. This uncertain part is used to calculate the normal operating thresholds.

The residual r and the uncertain part a are expressed as follows:

Jonction 1:

$$r = \sum e_{i_n} \tag{23}$$

$$a = \sum |w_i| \tag{24}$$

for 0 *junction*, e_{i_n} is replaced by f_{i_n}

Uncertain ARR part cannot be quantified perfectly, it is evaluated to generate a normal operation' threshold which satisfies the following inequality:

$$-a \leq r \leq a \tag{25}$$

The first ARR is generated from junction 1, connected to detector F_3.. This ARR is sensitive to the stopper at the level of the pump output (pipe radius variation). Knowing that the studied system is extremely perturbed, the expression of ARR_1 given by equation (26) takes into account the *Bernoulli* law.

$$ARR_1 : \begin{cases} r_1 = -\left(R_{z_{1n}}.F_3\right)^2 - \dfrac{A_T}{b.k_1.\rho_T.g}.\left(\dfrac{dP_1}{dt}\right) \\ \quad -\dfrac{k_2}{k_1} + P_1 - P_7 \\ a_1 = \left|\dfrac{w_{C_h}}{b.k_1}\right| + \left|\dfrac{w_{Rp}}{b.k_1}\right| + |w_{Rz_1}| \end{cases} \tag{26}$$

The second ARR is generated from the junction 0_h of the boiler model, for the detection of the mass leak:

$$ARR_2 : \begin{cases} r_2 = F_3 - \dfrac{d}{dt}\left(\rho_l.V_l + \rho_v.V_v\right) - F_{10} \\ a_2 = |w_{1C_{ht}}| \end{cases} \quad (27)$$

Finally, the third ARR is generated from the junction 0_t of the boiler model, in order to detect the thermo-resistance fault:

$$ARR_3 : \begin{cases} r_3 = F_3.c_{p_n}.T_2 + RS_n.Q_4 \\ \quad -\dfrac{d}{dt}\left(\rho_l.V_l.h_l + \rho_v.V_v.h_v - P_7.V_B\right) \\ \quad -Ra_n.\left(T_5 - T_a\right) - F_{10}.c_{v_n}.T_5 \\ a_3 = |w_{2C_{ht}}| + |w_{RS}| + |w_{Ra}| \\ \quad + |w_{RT_1}| + |w_{RT_2}| \end{cases} \quad (28)$$

4.1 Residuals sensitivity analysis

The residuals sensitivity analysis is made using the normalized partial derivative of the residual uncertain part compared to the parameter uncertainty, as shown in equation (29) (*M. A. Djeziri & al. (2007)* [6]).

$$\begin{cases} SI_{\delta_i} = \left|\dfrac{\delta_i}{a}.\dfrac{\partial a}{\partial \delta_i}\right| = \dfrac{|w_i|}{a} \\ a = \sum |w_i| \end{cases} \quad (29)$$

where δ_i is the multiplicative uncertainty on the parameter i, a is the ARR uncertain part. SI_{δ_i} is the sensitivity index according to δ_i. w_i is the fictive input according to the uncertainty on the parameter i.

A fault detectability indexes DI expressed in the equation (30) is defined as the ability of the residual to detect a physical fault. Two types of faults are considered: parameter fault (noted Y_i), and structural fault (noted Y_s)

· ARR generated from junction 1

$$\begin{cases} DI = Y_i.\,|e_{i_n}| + Y_s - \sum w_i \\ If\ DI \leq 0:\ \textit{Fault is not detectable} \\ If\ DI > 0:\ \textit{Fault is detectable} \end{cases} \quad (30)$$

or 0 *junction*, e_{i_n} is replaced by f_{i_n}

with DI the fault detectability index. Y_i is the fault detectable rate according to the parameter i. Y_s is the structural fault detectable value. $\sum w_i$ represents the sum of fictive inputs. e_{i_n} and f_{i_n} are respectively the nominal values of effort and flow given by the nominal parameter i.

Fault rate (Y_i) corresponds to an abnormal deviation of the parameter from its nominal value, which causes a failure of the system.

Structural fault (Y_s) causes a modification in the system structure, and consequently in its model. It creates an imbalance in the energetic assessments calculated in normal operation.

From equations (30) with considering $Y_s = 0$, the fault detectable rate Y_i on parameter i can be defined by the following equations (31)

· ARR generated from junction 1

$$Y_i > \frac{\sum |w_i|}{|e_{i_n}|} \quad (31)$$

for 0 *junction*, e_{i_n} is replaced by f_{i_n}

From equations (30), and by considering $Y_i = 0$, the structural fault detectable value can be defined by equation (32)

$$Y_s > \sum |w_i| \quad (32)$$

5. EXPERIMENTAL RESULTS

Experimental senary consists on the generation of the residuals and the normal operation thresholds using the acquired data from the real system. Four situations are considered:

1. Residuals generation without fault using the real sensors data; 2. Introduction of the first fault, by considering a stopper at the level of the pump output; 3. Introduction of the second fault as a fluid leak at the boiler level; 4. Introduction of the thermo-resistance breakdown.

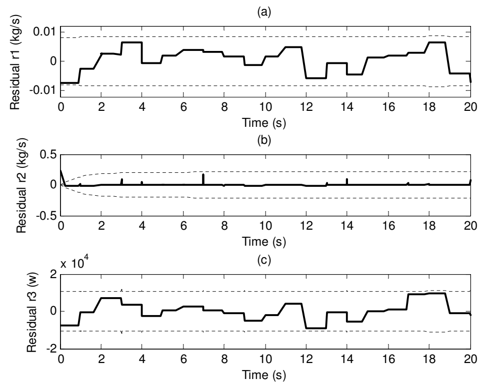

Fig. 4. The residuals r_1, r_2 and r_3 without faults.

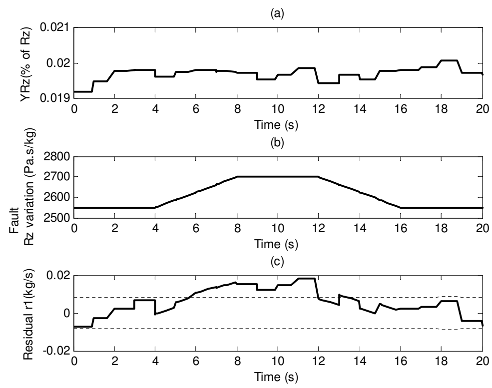

Fig. 5. (a): Y_{R_z}. (b): R_z variation. (c): Residual r_1

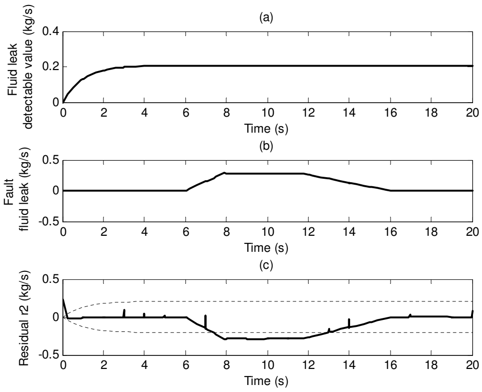

Fig. 6. (a): The fluid leak detectable value. (b): The introduced fault variation. (c): Residual r_2

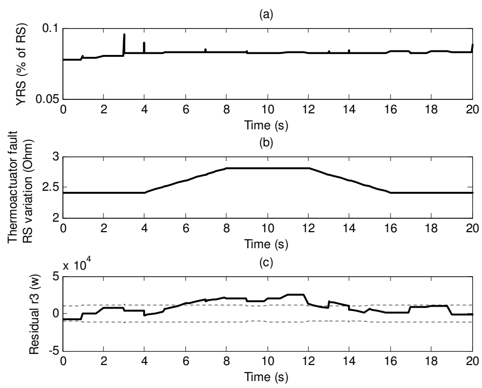

Fig. 7. (a): $Y_{R_{RS}}$. (b): RS variation. (c): Residual r_3

Figures 4-(a), (b) and (c) show respectively the residuals r_1, r_2 and r_3 without faults. The thresholds of normal operation are given with dot lines.

Fig. 5-(a) represents the fault detectable rate of R_z noted Y_{R_z}. Fig. 5-(b) shows the R_z nominal value, where a fault is introduced gradually between times $t = 4s$ and $t = 16s$. Fig. 5-(c) shows the reaction of the residual r_1 to this fault. The fault is detected when the rate of R_z deviation exceeds the detectable rate Y_{R_z}.

Fig. 6-(a) represents the fluid leak detectable value. Fig. 6-(b) shows the introduced fault, where the fluid leak is introduced gradually between times $t = 4s$ and $t = 16s$. Fig. 6-(c) shows the reaction of the residual r_2. The fault is detected when its energy being higher than that introduced by the whole uncertainties.

Fig. 7-(a) represents the fault detectable rate of RS noted Y_{RS}. Fig. 7-(b) shows the RS nominal value where a fault is introduced gradually between times $t = 4s$ and $t = 16s$. Fig. 7-(c) shows the reaction of the residual r_3 to this fault. The fault is detected when the rate of RS deviation exceeds the detectable rate Y_{R_z}.

6. CONCLUSION

Modeling and robust FDI of a steam generator are presented in this paper. Interactions of different phenomenon are taken into account by using the energetic properties of the bond graph tool. The nominal part of ARRs is perfectly separated from uncertain one. This latter is used to generate the adaptive thresholds of normal operation , then the parameter fault detectable rate and the structural fault detectable value are calculated. The use of bond graph as an integrated design tool for modeling and robust monitoring of energetic systems is well justified by the obtained results performances on the steam generator system.

REFERENCES

[1] O. Adort, D. Maquin, J. Ragot. (1999). 'Fault detection with model parameter structured uncertainties', European Control Conference ECC'99

[2] J. Armengol, L. T. Massuy'es, J. Vehi, J. L. de la Rosa. (2000). 'A survey on interval model simulators and their properties related to fault detection', Annual Review in Control. 24. pp. 31-39.

[3] K. Aström, R. Bell. (2000). 'Drum-boiler dynamics', Automatica. Vol 36. pp. 363-378.

[4] M. Basseville. (1998). 'On-board element fault detection and isolation using the statistical local approach', Automatica, vol. 34. No.11. pp.1359-1373.

[5] M. A. Djeziri, R. Merzouki, B. Ould Bouamama, G. Dauphin Tanguy (2006). 'Fault Detection of Becklash Phenomenon in Mechatronic System with Parameter Uncertainties using Bond Graph Approach', Proceeding of the 2006 IEEE International Conference on Mechatronics and Automation Luoyang, China. pp. 600-605.

[6] M. A. Djeziri, R. Merzouki, B. Ould Bouamama, G. Dauphin Tanguy (2007). ' Bond Graph Model Based For Robust Fault Diagnosis', Proceeding of the 2007 American Control Conference New York City, USA. pp. 3017-3022.

[7] L. J. de Miguel, L. F. Blazquez. (2005).'Fuzzy logic-based decision-making for fault diagnosis in a DC motor', Engineering Applications of Artificial Intelligence.Vol.18. pp. 423-450

[8] Z. Han ,W. Li , S. L. Shah. (2002). 'Fault detection and isolation in the presence of process uncertainties', 15th IFAC Wold Congress. pp.1887-1892.

[9] D. Henry, A. Zolghari. (2005). 'Norm-based design of robust FDI schemes for uncertain systems under feedback control: comparison of two approaches',In Press.

[10] K. Hsing-Chia, C. Hui-Kuo. (2004). 'A new symbiotic evolution-based fuzzy- neural approach to fault diagnosis of marine propulsion systems.' Engineering Applications of Artificial Intelligence, Vol.17. pp. 919-930